

Quasiparticle dynamics and in-plane anisotropy in $\text{YBa}_2\text{Cu}_3\text{O}_y$ system near onset of superconductivity

Y.-S. Lee,¹ Kouji Segawa,² Yoichi Ando,² and D. N. Basov¹

¹Department of Physics, University of California at San Diego, La Jolla, California 92093-0319

²Central Research Institute of Electric Power Industry, Komae, Tokyo 201-8511, Japan
(Dated: April 14, 2024)

We report on an infrared study of carrier dynamics within the CuO_2 planes in heavily underdoped detwinned single crystals of $\text{YBa}_2\text{Cu}_3\text{O}_y$. In an effort to reveal the electronic structure near the onset of superconductivity, we investigate the strong anisotropy of the electromagnetic response due to an enhancement of the scattering rate along the a -axis. We propose that the origin of this anisotropy is related to a modulation of the electron density within the CuO_2 planes.

PACS numbers: 74.25.Gz, 74.72.Bk

The physics of Mott-Hubbard (MH) insulators is at the focus of current research in part because of a variety of enigmatic ground states that can be initiated through doping of these systems.¹ A particularly interesting example is high- T_c superconductivity which is triggered by doping of MH insulating cuprates and is believed to originate from strong correlations among the doped holes.² To elucidate the unconventional superconductivity, it is therefore imperative to understand the nature of the conducting state derived from the Mott insulator. Thus motivated, we have carried out systematic studies of the electromagnetic response of a prototypical high- T_c superconductor $\text{YBa}_2\text{Cu}_3\text{O}_y$ (YBCO) over a broad region of the phase diagram across the antiferromagnetic (AF) transition and onset of superconductivity.

One of the intriguing properties of heavily underdoped YBCO is the in-plane anisotropy in the DC resistivity.³ This effect is likely to be distinct from the anisotropy seen in the YBCO system near optimal doping.^{3,4,5} The latter is attributed to the one-dimensional (1-D) Cu-O chains along the b -axis which are capable of contributing both to the DC transport and to the superfluid density,^{6,7} provided the disorder in the chains is weak. Although the direct role of chains in the anisotropy of weakly doped phases has not been explicitly ruled out, this scenario is rather remote because considerable defects in the chains are inevitable in oxygen deficient crystals. In searching for alternative mechanisms of the anisotropy, it is prudent to take into consideration anisotropic transport and infrared response within the CuO_2 plane in a nearly tetragonal chain-free cuprate $\text{La}_{2-x}\text{Sr}_x\text{CuO}_4$ (LSCO).^{3,8} It has been argued that the directional dependence of quasiparticle dynamics in LSCO may be related to the intrinsic tendency of doped MH insulators towards spin and/or charge self-organization in real space. Similar spin/charge modulation has also been observed in YBCO from neutron and x-ray scattering experiments.^{9,10,11,12} Infrared (IR) spectroscopy is ideally suited for elaborating in-plane anisotropy in the heavily underdoped YBCO because reflectance measurements with polarized light are capable of separating the contribution of the 1-D chains from the response of the CuO_2 planes.

Here we report on the study of the optical spectra for

the heavily underdoped YBCO with oxygen contents $y = 6.30, 6.35, 6.40$, and 6.43 , grown by a conventional flux method and detwinned under uniaxial pressure.¹³ The $y = 6.43$ and 6.40 samples are superconducting with transition at $T_c = 13$ K and 2 K, respectively, determined from the DC resistivity measurement shown in the inset of Fig. 1(a).¹³ At lower dopings the ground state of YBCO is antiferromagnetic.^{14,15} Annealing under the uniaxial pressure aligns chain segments along the b -axis in

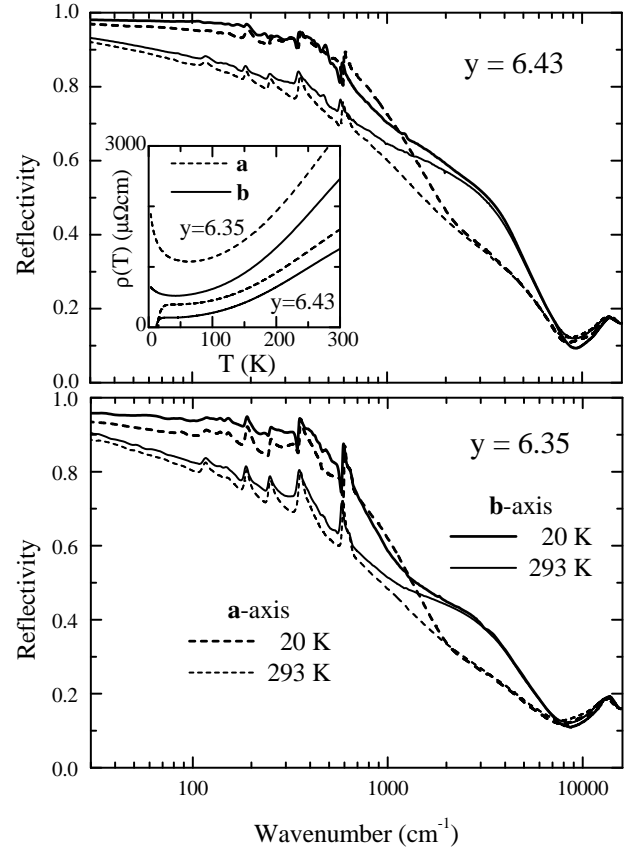


FIG. 1: T-dependent $R(\omega)$ for (a) $y = 6.43$ and (b) $y = 6.35$. Inset in (a) shows DC resistivity curves for $y = 6.43$ and 6.35 crystals.

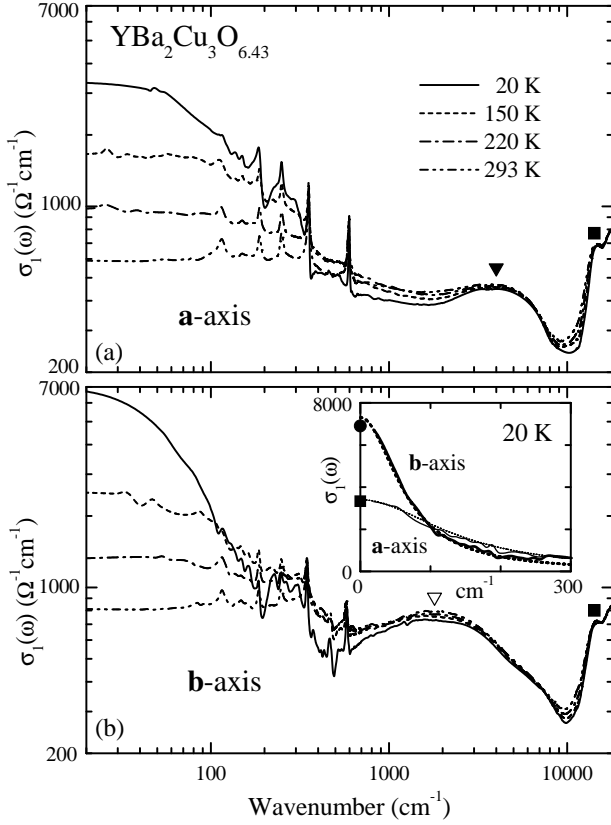


FIG. 2: T-dependent $\sigma_1(\omega)$ of the $y = 6.43$ YBCO along (a) the a-axis and (b) the b-axis. The circle and the square symbols represent the positions of MIR resonances and CT excitations, respectively. In the inset in (b), the $\sigma_1(\omega)$ with the phonon subtracted are used for the Drude fitting (the dotted lines). Note that the fits are adequate for the frequency range exceeding parameters. The symbols represent the DC resistivity values.

non-superconducting YBCO crystals. All samples show an in-plane anisotropy in resistivity, with higher conductivity along the b-axis.³ Resistivity spectra $R(\omega)$ at near normal incidence were measured with polarized light at frequencies from 20 to 48000 cm^{-1} and at temperatures from 20 to 293 K. According to the Hagen-Rubens relation, $R(\omega) \propto \frac{\rho_{DC}}{\omega}$, where ρ_{DC} is the DC resistivity value. As shown in Fig. 1, the far-IR resistivities along the b-axis are higher than those along the a-axis, which is consistent with the anisotropy in the DC resistivity. In addition, the mid-IR $R(\omega)$ is enhanced along the b-axis. This behavior is associated with the optical response of chain fragments aligned along the b-axis, which will be described below. With T decreasing, the low frequency $R(\omega)$ increase considerably whereas the change in the mid-IR is negligible. The complex optical conductivity spectra, $\sigma(\omega) = \sigma_1(\omega) + i\sigma_2(\omega)$, were obtained from the measured $R(\omega)$, using Kramers-Kronig (KK) transformation. The KK-derived results are consistent with those obtained independently by spectroscopic ellipsometry in the near-IR and visible region.

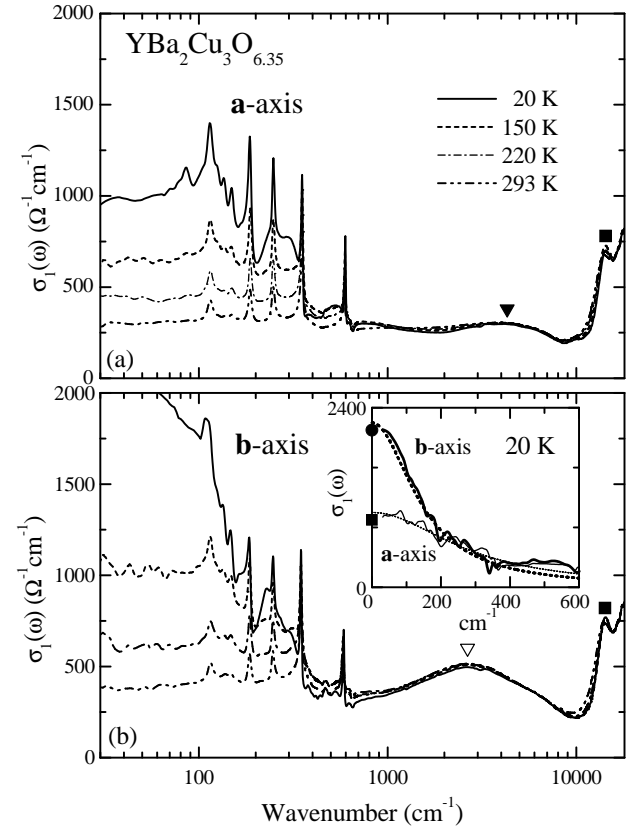


FIG. 3: T-dependent $\sigma_1(\omega)$ of the $y = 6.35$ YBCO in (a) the a-axis and (b) the b-axis. The circle and the square symbols represent the positions of the MIR resonances and the CT excitations, respectively. In the inset in (b), the $\sigma_1(\omega)$ with the phonon subtracted are used for the Drude fitting (the dotted lines). The symbols represent the DC resistivity values.

Figures 2(a) and 2(b) show the dissipative part of the optical conductivity $\sigma_1(\omega)$ for the $y = 6.43$ sample along the a- ($\sigma_{1,a}(\omega)$) and the b-axis ($\sigma_{1,b}(\omega)$), respectively. The optical spectra in both polarizations show qualitatively common features, including a charge transfer (CT) excitation seen around 14,000 cm^{-1} and substantial electronic spectral weight within the CT gap. The intra-gap spectral weight is comprised of two separate absorption features: a coherent mode at lowest frequencies ($\omega < 600 \text{ cm}^{-1}$) followed by a mid-IR resonance. The distinct character of the two absorption features is most evident in the low-T data: the mid-IR structure is virtually independent of T, whereas the coherent mode significantly narrows at low-T leading to a minimum in $\sigma_1(\omega)$ between the two components. This two-component optical conductivity is also observed in the other YBCO samples (Fig. 3) and is a general characteristic of weakly doped cuprates.¹⁶ Apart from this electronic contribution, the conductivity spectra also reveal sharp peaks due to IR-active phonons. The phonon frequencies show noticeable differences in the a- and b-axis data confirming that the studied samples are detwinned.

Coherent low- ω features in the optical response of all

TABLE I: Summaries of the Drude fitting parameters, the plasma frequency ω_p and the scattering rate γ , for $\lambda_c(\lambda)$ of $\text{YBa}_2\text{Cu}_3\text{O}_{y=6.30}$ at 20 K along the a- and b-axis. For $y = 6.30$, we used the data at 80 K just above the onset T_c of an insulating-like state. Using the measured Hall coefficient at 300 K, the mean free path λ at the corresponding T_c are also estimated with a three dimensional free electron model.

y	ω_p (cm^{-1})		γ (cm^{-1})		λ (Å)	
	a	b	a	b	a	b
6.43	5250	5340	135	65	57	121
6.40	4350	4420	210	105	31	64
6.35	4100	4300	280	140	24	52
6.30	3630	3890	430	270	14	25

YBCO crystals are well described with the AC Drude formula, $\epsilon(\omega) = (\omega_p^2 / (\omega^2 - \gamma^2))$, where ω_p and γ are the plasma frequency and the scattering rate of carriers, respectively. The fits are presented with the dotted lines in the insets of Figs. 2(b) and 3(b) with the fitting parameters reported in Table I. Interestingly, the Drude description holds for the $y = 6.35$ crystal at 20 K, which is less than the Neel temperature for this particular composition.¹⁷ The coherent response of the $y = 6.30$ sample at the lowest T is modified compared to the simple Drude formula: the electronic conductivity reveals a weak peak near 100 cm^{-1} suggestive of the carrier localization.

An outstanding property of heavily underdoped YBCO is anisotropy in the coherent modes with a marked increase of the conductivity along the b-direction. A quick inspection of the Drude parameters in Table I reveals that this effect is primarily produced by the anisotropy of γ whereas the anisotropy of ω_p is fairly small. An independent confirmation of this finding is provided by an examination of the electronic spectral weight $N_e(\omega) = \frac{1}{\omega} \text{Im}[\epsilon(\omega)]$. The oscillator strength sum rule suggests that integration over the frequency region of the coherent mode ($\omega \approx 600 \text{ cm}^{-1}$) provides an accurate estimate of ω_p^2 . The spectra presented in Figs. 4(a) and 4(b) show that the anisotropy of the plasma frequency $\omega_{p,b} = \omega_{p,a} \sqrt{N_{e,b}/N_{e,a}}$ does not exceed 1.12 for the $y = 6.35$ sample and 1.07 for the $y = 6.43$ specimen at $\omega \approx 600 \text{ cm}^{-1}$. These results are quite comparable with the Drude fitting results in Table I. As $\omega \rightarrow 0$, the $N_{e,b}(\omega) = N_{e,a}(\omega)$ values approach the ratio of the DC conductivities $\sigma_{c,b} = \sigma_{c,a}$, indicating that the optical results are also consistent with the transport data. The dominant role of γ in the anisotropic carrier dynamics of YBCO is further confirmed by the data in the inset of Fig. 4(b) where we display the T -dependent $\sigma_{a=b}$ extracted from Drude fits along with the DC resistivity ratios $\sigma_{c,a} = \sigma_{c,b}$. Close agreement between the two data sets establishes that the significant anisotropy in σ is primarily responsible for the resistivity anisotropy within the CuO_2 plane in weakly doped YBCO compounds.

What is the origin of the anisotropic scattering?

Searching for plausible causes of this enigmatic effect, it is imperative to access the possible role of Cu-O chains as well as that of the orthorhombicity of YBCO. As pointed out above, highly ordered chains in the (nearly) stoichiometric $\text{YBa}_2\text{Cu}_3\text{O}_{6.95}$ and $\text{YBa}_2\text{Cu}_4\text{O}_8$ crystals contribute directly to DC transport.⁷ This contribution is reflected in strong enhancement of the b-axis plasma frequency and in the anisotropy of $\sigma_{c,b} = \sigma_{c,a}$ that appears to scale with $\omega_{p,b} = \omega_{p,a}$.^{6,7} Notably, YBCO crystals with $T_c \sim 90 \text{ K}$ containing significant disorder on the chain sites (due to non-optimized growth and/or annealing conditions) do not reveal substantial DC anisotropy.¹⁸ In this case, the b-axis conductivity shows a strong resonance at $\omega \approx 1500 - 2000 \text{ cm}^{-1}$, usually assigned to carrier localization in the Cu-O chain segments.^{19,20,21} Examining the mid-IR response of the weakly doped YBCO in light of these earlier results, we first note substantial anisotropy of the mid-IR conductivity which can be readily traced in $R(\omega)$. The mid-IR resonances in the a-axis spectra are located at $\approx 4200 \text{ cm}^{-1}$ without any significant y -dependence in the heavily underdoped region. This feature reflects the intrinsic electronic structure of the doped CuO_2 planes and is rather insensitive to a particular host material.^{8,16,22} On the other hand, the mid-IR resonances in the b-axis are located at much lower frequencies: $\approx 1700 \text{ cm}^{-1}$ at $y = 6.43$ and $\approx 3100 \text{ cm}^{-1}$ at $y = 6.30$. The spectral weight of these b-axis features significantly exceeds that of the resonances observed in the a-axis spectra. To obtain further insight into the chain response, we checked $\lambda_{b,b}(\omega) - \lambda_{b,a}(\omega)$ which are attributable to the chains. These differential spectra reveal an over-damped oscillator at $1500 - 2600 \text{ cm}^{-1}$ and are comparable to the disordered chain response in the YBCO system at higher doping.^{19,20,21} As y decreases and the density of oxygen defects in the chains is enhanced, the peaks shift to higher frequency while their spectral weight is reduced. These observations are in accord with the theoretical analysis of the localized state of the oxygen-deficient chains in YBCO system.²³ The notion of carrier localization in the Cu-O chain segments is consistent with the experimental fact that no significant anisotropy in ω_p is found in our data. We therefore conclude that the chains in the studied specimen are unable to maintain conductivity in the DC or low- ω limit.

We now turn to the possible impact of orthorhombicity on anisotropic quasiparticles dynamics. As pointed out above, the bulk orthorhombicity of the studied specimen is supported by the anisotropy of the phonon frequencies. Their doping trends are shown in Fig. 4(c) and 4(d), where we display the y -dependence of the stretching mode frequencies ω_{ph} , which are most sensitive to the variation of the lattice constants.²⁴ Comparing the $\omega_{ph,a} = \omega_{ph,b}$ ratios with the anisotropy of the DC conductivity (or AC conductivity in the $\omega \rightarrow 0$ limit), one notices that the latter increases as the YBCO system progresses towards the tetragonal phase ($\omega_{ph,a} = \omega_{ph,b} \rightarrow 1$).¹⁴ Interestingly, the higher $\omega_{ph,a}$ values indicate that the lattice constant in the a-axis is shorter than that in the

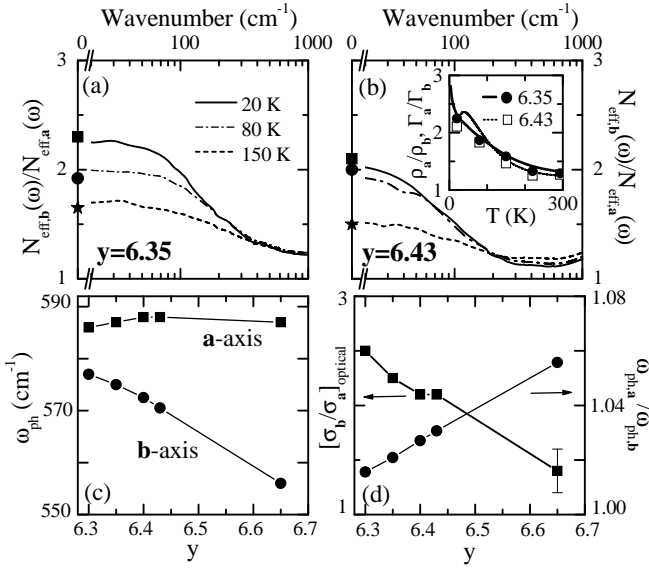


FIG. 4: Top panels: T-dependent $N_{e,b}(!) = N_{e,a}(!)$ at (a) $y = 6.30$ and (b) $y = 6.43$. The square, the circle, and the star symbols correspond to the measured $\rho_{DC,b} = \rho_{DC,a}$ values at 20 K, 80 K, and 150 K, respectively. Low panels display the evolution of the anisotropy of the phonon modes. (c) At 293 K, the frequencies of phonons positioned at the highest frequency at $y = 6.30, 6.35, 6.40, 6.43$, and 6.65 . (d) y-dependence of $\omega_{ph,a} = \omega_{ph,b}$ and $[\sigma_b/\sigma_a]_{\text{optical}} \lim_{\omega \rightarrow 0} \omega_{ph} = \omega_{ph}$. For $y = 6.65$, we choose the value at 65 K just above T_c . In the inset of (b), the dotted and the solid lines represent the $\omega_{ph,a} = \omega_{ph,b}$ curves at $y = 6.43$ and $y = 6.35$, respectively. The square ($y = 6.43$) and the circle ($y = 6.35$) symbols correspond to the T-dependent $\omega_{ph,a} = \omega_{ph,b}$ values multiplied by 1.05 and 1.1, respectively.

b-axis. According to the tight binding picture, one would expect to find an enhancement of the electronic spectral weight (proportional to hopping integrals) in the polarization of E vector along the shorter axis, which is not realized in the N_e analysis discussed above. We therefore conclude that structural orthorhombicity can be safely excluded from factors defining anisotropic electronic response of weakly doped YBCO.

What are the microscopics behind the anisotropic scattering within the CuO_2 plane leading to an enhancement of the conductivity along the direction of chain segments? It is rather unlikely that the chains directly contribute to the anisotropic in-plane because scattering by the out-of-plane defects involves only a small momentum transfer which is of little consequence for transport phenomena.²⁵ With this possibility being eliminated it is appealing to explore indirect impact of chains through an "in print" of the charge density in the CuO_2 planes recently observed through both x-ray experiments¹² and nuclear resonance.²⁶ These latter studies indicate that chain segments act as a template to induce (stripe-like) charge modulation in the neighboring planes. This modulated state may act as a scattering source enhancing the carriers propagating along the modulation direction (a-

axis) in accord with our observations. We note that the ordered chain segments form "patches" elongated along the b-axis with the aspect ratio $\sim 3:1$,²⁷ which are comparable to the anisotropy of the mean free path within the CuO_2 plane reported in Table I. The charge modulation may be related to the tendency of doped Mott insulators to form self-organized stripe-like phases when both spin and charge ordering are expected. Indeed the T-dependence of the anisotropy of ρ appears to be in accord with that of the strength of the stripe-related magnetic structure seen in neutron scattering measurements.^{9,10}

The experiments reported here provide important insights into the nature of the modulated electronic state. First, the charge modulation appears to be only loosely coupled to the lattice because no phonon zone-folding effects can be readily identified within the signal-to-noise ratio in our data.²⁸ Second, the amplitude of the charge modulations must be rather weak because the electronic transport within the CuO_2 planes retains its two-dimensional character even at the lowest T where the anisotropy is maximized. This anisotropic transport in the metallic state has to be contrasted with the case of the weakly doped LSCO system. In the latter materials, the anisotropic conductivity is accompanied with the development of localization peak in $\rho_{\parallel}(!)$ spectra that is in qualitative agreement with the notion of 1-D confinement of carrier motion.⁸ A common aspect of both cuprates is that the c -plane structural distortions (chain fragments in YBCO and octahedra tilts in LSCO) appear to play a preeminent role in stabilizing charge non-uniformity within the CuO_2 planes. Charge modulations triggered by these two stabilizing methods are different: enhanced electron density is collinear with respect to Cu-O bonds in the case of YBCO and diagonal in LSCO. Nevertheless, in both cases we observe an enhancement of the far-IR conductivity across the modulation direction signaling that this effect is the intrinsic property of weakly doped CuO_2 planes. We remark that in YBCO systems the (stripe-like) charge modulations are found here to coexist with superconductivity in contrast to the experimental situation in LSCO.²⁹ This observation is significant because the stripes framework offers an interesting perspective on the pairing mechanism in high- T_c cuprates.³⁰

In conclusion, our infrared studies of heavily underdoped YBCO reveal that the in-plane optical spectra below the charge transfer gap are comprised of the well-separated D_{nd}-like coherent mode and mid-IR resonance. We observe substantial anisotropy of the electronic transport within the CuO_2 planes due to the enhanced scattering rate along the a-axis. The chain segments and their ordering appear to play a profound role in the anisotropic transport by imprinting charge modulations in the CuO_2 planes.

We wish to thank S. A. Kivelson for his fruitful discussions and valuable comments. This research was supported by the US Department of Energy Grant No. DE-FG0300ER45799. Y.-S.L. was partially supported by the Post-doctoral Fellowship Program of Korea Science En-

- ¹ M. Imada, A. Fujimori, and Y. Tokura, *Rev. Mod. Phys.* **70**, 1039 (1998).
- ² J. Orenstein and A. J. Millis, *Science* **288**, 468 (2000), and references therein.
- ³ Yoichi Ando, Kouji Segawa, Seiki Komiyama, and A. N. Lavrov, *Phys. Rev. Lett.* **88**, 137005 (2002).
- ⁴ T. A. Friedmann, M. W. Rabin, J. Giapintzakis, J. P. Rice, and D. M. Ginsberg, *Phys. Rev. B* **42**, 6217 (1990).
- ⁵ R. Harris, A. Hosseini, Saeid Kamal, P. Dosanjh, Ruixing Liang, W. N. Hardy, and D. A. Bonn, *Phys. Rev. B* **64**, 64509 (2001).
- ⁶ D. N. Basov, R. Liang, D. A. Bonn, W. N. Hardy, B. Dabrowski, M. Quijada, D. B. Tanner, J. P. Rice, D. M. Ginsberg, and T. Timusk, *Phys. Rev. Lett.* **74**, 598 (1995).
- ⁷ P. Wachter, B. Bucher, and R. Pittini, *Phys. Rev. B* **49**, 13164 (1994).
- ⁸ M. Dumm, Seiki Komiyama, Yoichi Ando, and D. N. Basov, *Phys. Rev. Lett.* **91**, 077004 (2003).
- ⁹ Pengcheng Dai, H. A. Mook, and F. Dogan, *Phys. Rev. Lett.* **80**, 1738 (1998).
- ¹⁰ H. A. Mook and F. Dogan, *Nature* **401**, 145 (1999).
- ¹¹ H. A. Mook, Pengcheng Dai, F. Dogan, and R. D. Hunt, *Nature* **404**, 729 (2000).
- ¹² Zahinul Islam, S. K. Sinha, D. Haskel, J. C. Lang, G. Srajer, B. W. Veal, D. R. Haefer, and H. A. Mook, *Phys. Rev. B* **66**, 092501 (2002); Zahinul Islam, X. Liu, S. K. Sinha, J. C. Lang, S. C. Moss, D. Haskel, G. Srajer, P. Wochner, D. R. Lee, D. R. Haefer, and U. Welp, cond-mat/0312622.
- ¹³ Kouji Segawa and Yoichi Ando, *Phys. Rev. Lett.* **86**, 4907 (2001).
- ¹⁴ J. D. Jorgensen, B. W. Veal, A. P. Paulikas, L. J. Nowicki, G. W. Crabtree, H. Claus, and W. K. Kwok, *Phys. Rev. B* **41**, 1863 (1990).
- ¹⁵ A. N. Lavrov, Y. Ando, K. Segawa, and J. Takeya, *Phys. Rev. Lett.* **83**, 1419 (1999).
- ¹⁶ T. Timusk and D. B. Tanner, in *Physical Properties of High Temperature Superconductors III*, edited by D. M. Ginsberg, World Scientific, Singapore, 1992, Chap. 5.
- ¹⁷ The low frequency localization mode in the FIR region, which is clearly observed at $y = 6:30$, is expected to occur far below 20 K, consistent with the insulating-like behavior in (T).
- ¹⁸ U. Welp, S. Fleshler, W. K. Kwok, J. Downey, Y. Fang, G. W. Crabtree, and J. Z. Liu, *Phys. Rev. B* **42**, 10189 (1990).
- ¹⁹ S. L. Cooper, D. Reznik, A. Kotz, M. A. Karlow, R. Liu, M. V. Klein, W. C. Lee, J. Giapintzakis, D. M. Ginsberg, B. W. Veal, and A. P. Paulikas, *Phys. Rev. B* **47**, 8233 (1993).
- ²⁰ L. D. Rotter, Z. Schlesinger, R. T. Collins, F. Holtzberg, C. Field, U. W. Welp, G. W. Crabtree, J. Z. Liu, Y. Fang, K. G. Vandervoort, and S. Fleshler, *Phys. Rev. Lett.* **67**, 2741 (1991).
- ²¹ K. Takenaka, Y. Imamura, K. Tamasaku, T. Ito, and S. Uchida, *Phys. Rev. B* **46**, 5833 (1992).
- ²² S. Uchida, T. Ido, H. Takagi, T. Arima, Y. Tokura, and S. Tajima, *Phys. Rev. B* **43**, 7942 (1991).
- ²³ R. Franco and A. A. Alija, *Phys. Rev. B* **67**, 172507 (2003), and references therein.
- ²⁴ S. Tajima, T. Ido, S. Ishibashi, T. Itoh, H. Eisaki, Y. Mizuo, T. Arima, H. Takagi, and S. Uchida, *Phys. Rev. B* **43**, 10496 (1991).
- ²⁵ Hae-Young Kee, *Phys. Rev. B* **64**, 012506 (2001).
- ²⁶ B. Grevin, Y. Berthier, and G. Collin, *Phys. Rev. Lett.* **85**, 1310 (2000).
- ²⁷ R. Liang, D. Bonn, and W. N. Hardy, *Physica C* **336**, 57 (2000); R. Liang, D. A. Bonn, W. N. Hardy, J. C. Wynn, K. A. Moler, L. Lu, S. Larochelle, L. Zhou, M. Grevin, L. Lurio, and S. G. J. Mochrie, *Physica C*, **383**, 1 (2002).
- ²⁸ It is desirable to improve the S/N ratio through ellipsometric experiments. The latter studies are indicative of the additional phonon structure in the b-axis spectra of the $y = 6:95$ phase: C. Bernhard, T. Holden, J. Hummel, D. Munzar, A. Golnik, M. K. Kaser, Th. Wolf, L. Carr, C. Homes, B. Keimer, and M. Cardona, *Solid State Communications* **121**, 93 (2002).
- ²⁹ N. Ichikawa, S. Uchida, J. M. Tranquada, T. Niemoller, P. M. Gehring, S.-H. Lee, and J. R. Schneider, *Phys. Rev. Lett.* **85**, 1738 (2000).
- ³⁰ V. J. Emery, S. A. Kivelson, and O. Zachar, *Phys. Rev. B* **56**, 6120 (1997).